Original Article

Development of droplet entrainment and deposition models for horizontal flow

Joshua Kim Schimpf [a], Kyung Doo Kim [b, *], Jaeseok Heo [b], Byoung Jae Kim [c]

[a] Advanced Nuclear Systems Engin., University of Science and Tech., 176 Gajeong-dong, Yuseong-gu, Daejeon, South Korea
[b] Thermal Hydraulics Safety Research Division, 989-111 Daedeok-daero, Yuseong-gu, Daejeon, 305-353, South Korea
[c] School of Mechanical Engineering, Chungnam National University, 99 Daehak-ro, Yuseong-gu, Daejeon 34134, South Korea

A B S T R A C T

Models for the rate of atomization and deposition of droplets for stratified and annular flow in horizontal pipes are presented. The entrained fraction is the result of a balance between the rate of atomization of the liquid layer that is in contact with air and the rate of deposition of droplets. The rate of deposition is strongly affected by gravity in horizontal pipes. The gravitational settling of droplets is influenced by droplet size: heavier droplets deposit more rapidly. Model calculation and simulation results are compared with experimental data from various diameter pipes. Validation for the suggested models was performed by comparing the Safety and Performance Analysis Code for Nuclear Power Plants calculation results with the droplet experimental data obtained in various diameter horizontal pipes.
© 2018 Korean Nuclear Society, Published by Elsevier Korea LLC. This is an open access article under the CC BY-NC-ND license (http://creativecommons.org/licenses/by-nc-nd/4.0/).

1. Introduction

Steam binding is an important phenomenon that can affect the peak cladding temperature during a loss of coolant accident. The prediction of the rate of atomization from the liquid layer and the rate of deposition of droplets must be precise and is directly linked with the amount of entrained droplets that reach the steam generator before vaporization. Gas—liquid flow may occur in the PWR (Pressurized Water Reactor) hot leg and is an important component process that is associated with this accident.

The nuclear industries and research institutes in Korea have developed a thermal-hydraulic analysis code for safety analysis of PWRs, named Safety and Performance Analysis Code for Nuclear Power Plants (SPACE). The SPACE code adopts advanced physical modeling of two-phase flows: mainly two-fluid three-field models comprised of a gas, a continuous liquid, and a droplet field. Two-fluid three-field modeling allows the explicit simulation of the steam-binding phenomena. In this study, models for rate of entrainment and deposition are suggested and implemented in the SPACE code. Results of simulation are then compared with experimental data from horizontal pipes of various dimensions.

Prediction of the liquid field mass distribution in the liquid layer and dispersed droplets is critical; therefore, this distribution is the figure of merit for this study. This study is a further advancement of the previous study *Droplet Entrainment and Deposition in Horizontal Stratified Two-Phase Flow* [1]. The newly proposed models differ in that the diameter term is more accurately predicted, allowing better predictions for the gravitational settling term. In addition, developing regions are considered with respect to the interfacial area term modeling between liquid layer and gas core. Overall, predictions over a wider range of experimental facilities were improved on previous approximations.

2. Droplet entrainment and deposition experiments

The two-phase flow behaviors of interest in this study include droplet entrainment and deposition in the horizontal annular and stratified flow regime. Measurements of droplet entrainment for air and water flows in horizontal pipe experiments from the studies by Williams (0.095 m) [2], Dallman (0.0231 m) [3], Laurinat et al. (0.0508 m) [4], Mantilla (0.0486 m) [7], and REGARD (0.24 m) [6] are examined. Horizontal annular flow exists under flow conditions in which gas velocities are high and liquid film exists around the perimeter of the pipe. Horizontal stratified flow occurs at lower gas velocities, and liquid film may occupy the lower portion of the pipe. Both flow regimes are studied in this article,

* Corresponding author.
E-mail address: kdkim@kaeri.re.kr (K.D. Kim).

and the effects of gravity and pipe diameter on droplet behavior are considered.

The entrained ratio is the balance of the rate of atomization of the liquid film, Γ_E, and the rate of deposition of droplets, Γ_D. At the contact point of gas and liquid entering a pipe in two-phase flow, a developing region occurs in which the mass flow of the droplets will increase until the rate of atomization equals that of deposition. The point at which entrainment is equal to deposition is considered a fully developed flow, $\Gamma_E = \Gamma_D$. Five experiments were selected to measure entrainment ratios for horizontal flow conditions. RE-GARD experiment was performed at CEA Grenoble to study both developing and developed flow for a pipe with diameter of 0.24 m. Williams [2], Dallman [3], and Laurinat et al. [4] performed experiments at the University of Illinois at Urbana–Champaign and observed a fully developed flow for pipe diameter size ranges of 0.0254–0.095 m. In addition, a separate study with droplet measurements for a horizontal flow in a 0.0486-m diameter pipe was performed by Ivan Mantilla at the University of Tulsa.

Williams, Dallman, and Laurinat et al. studied two-phase flow at a range of various scales. The facility has the capability to experiment under pipe diameter sizes of 2.54 cm, 5.08 cm, 7.62 cm, and 9.53 cm and the pipe lengths ranging up to 26.5-m long. The pressure at the test section varied between experiments, such that P=116–212 kpa.

The REGARD facility is another experimental facility developed to study two-phase flows in a hot leg geometrical configuration. The facility differs in that it is specifically designed to study horizontal stratified flows as opposed to Williams' prior investigation of horizontal annular and stratified flows [2]. The experiment used liquid water and air, both at 30°C, at a pressure slightly below 150 kPa. The pipe had a diameter of 0.24 m. Axial measurement capabilities were utilized between L/D ratios 3.8 and 11.6. When compared with other facilities, this facility is the closest in geometrical scale, by far, to actual PWR geometries [6].

Mantilla's experimental facility consisted of a 2-inch flow loop of clear PVC (PolyVinyl Chloride) with an inner diameter of 0.0486 m. For every set of experimental flow condition runs, the pressure was constant at 206.8 kPa. Inlet liquid and gas mass flow rates were maintained constant for each of the experimental runs. Fluid temperatures were also maintained at around 21°C. This experimental facility is a small-scale one that covers droplet entrainment measurements for horizontal flow [7]. Table 1 shows the conditions for the range of experiments used in developing the entrainment and deposition modeling.

3. Previous studies for droplet entrainment and deposition modeling

There are a vast range of existing studies on droplet behavior, including deposition and entrainment modeling. During the first stages of research in this field, vertical pipes were studied because droplet deposition behavior is a less complex phenomenon as opposed to horizontal flow. In vertical flow, droplet concentration profiles are usually uniform. Previous developed models used an approach that predicts the free flight rate at which droplets will be deposited in the liquid film.

Later research expanded toward horizontal pipes covering annular and stratified annular flow regimes. Attempts were made to model the deposition behavior; however, these were limited to one experimental facility for the development of the deposition models. This study includes a deposition model that considers gravitation and can be applied to different scale pipe diameter experiments.

Experimental data were obtained from the aforementioned facilities. Data were further analyzed and validated with the SPACE simulation program. On simulation, existing models for entrainment and deposition did not match well against the experimental data. SPACE used deposition modeling from vertical flows that are not applicable to horizontal flow because gravity was not considered. The deposition model for vertical flows was developed by McCoy and Hanratty [8] from a range of experiments that studied the rate at which injected particles deposit at the wall of a pipe. The droplet diameter has a major influence on the rate of deposition for both gravitational settling and turbulent diffusion. However, the previous deposition experiments did not have enough data for the larger droplet diameters that were observed in the horizontal flow experiments.

In the first stages of development of droplet deposition modeling in horizontal flow, Williams et al. (1996) considered the effect of gravity. The experiments showed that different pipe diameter sizes had significant differences in droplet concentration distributions and liquid film distributions. The author attributed this difference to the influence of gravity. In addition, this effect of gravity was also observed in the REGARD experiment facility. The author defined these distributions with parameters "asymmetry" and "symmetry". As the pipe sizes increased, liquid film and droplet distributions became nonuniform among the cross sections of a pipe and were considered asymmetric, whereas small diameter pipe experiments saw more uniform symmetric distributions under similar flow conditions.

Before the study by Williams et al. [9], other experiments measuring the deposition rate for droplets in horizontal pipes also observed strong effects of gravity. In the smallest scale experiment, Alexander and Coldren [10] observed symmetric profiles. Larger scale experiments, such as those by Namie and Ueda [11] and McCoy and Hanratty [8], found asymmetric concentration distributions. Visual observations and measurements suggested that almost all the deposition was occurring at the bottom wall of the pipes. More consistent measurements and observations of these trends were shown in the study by Anderson and Russell [12]; they measured the circumferential variation of interchange and found that nearly 90% of the interchange occurred at the bottom half of the pipe. In all these experimental studies, it is clear that gravity has a significant effect on the droplet behavior.

Table 1
Experiments used for entrainment modeling.

	Williams (1990)	Laurinat (1984)	Dallman (1978)	Mantilla (2008)	REGARD (2012)
Fluids	Air–water	Air–water	Air–water	Air–water	Air–water
D (m)	0.0953	0.0508	0.0231	0.0486	0.24
J_g (m/s)	26–88	11–131	15–88	21–84	19–38
W_L (kg/s)	0.12–0.86	0.033–0.97	0.003–0.25	0.006–0.188	0.83–1.66
$\rho_g kg/m^3$	1.3–1.85	2.05	1.26–2.75	2.48	1.75
No. of boundary conditions	29	52	114	22	8
Pressure (kPa)	116	212	212	207	150

The distribution of the liquid film can be characterized by the Froude number. The definition of the Froude number is given by:

$$F_r = \frac{U_g}{\sqrt{D*g}} \tag{1}$$

The Froude number is a dimensionless number that can show trends between the liquid distribution of the liquid film and droplet distribution in a cross section of a horizontal pipe. Table 2 shows the Froude number calculations for the set of air velocities under the REGARD, Mantilla, and Williams experiments.

Air velocities of over 45 m/s for Williams experiment experienced Froude numbers above 50, and the liquid film was more symmetric as annular flow regimes were approached. As flows approach higher air speeds and Froude numbers, evenly distributed concentration profiles, similar to vertical flows, can be observed. Cases in which Froude numbers exceed the suggested value,$Fr=190$, occur when the concentration profiles are nearly uniform; however, the entrained fraction approaches unity at these values. The entrained fraction is defined by the ratio of the mass flow rate of droplets to the total mass flow rate of liquid, where

$$E = \frac{W_{LE}}{W_L} \tag{2}$$

The effect of an increase of pipe diameter size is closely related to droplet behavior and should be accounted for in deposition modeling. There have been numerous past studies on droplet behavior in horizontal flow; however, few have been published that cover horizontal stratified flow. Previous experimental facilities have small pipe diameters and do not cover stratified flow because droplet entrainment is negligible at the flow conditions for which stratified flow occurs in a small-scale pipe.

3.1. Drop size literature review

A central problem in analyzing two-phase flows is the prediction of the drop size. The drop size influences the rate of deposition, and therefore, an accurate prediction of this parameter is necessary for successful deposition modeling. Tatterson et al. [14] gave the following estimate of the effects of the system variables on the drop size:

$$d_d = D^{0.5} \left(\frac{\sigma}{\rho_g \left(U_g\right)^2 f_s} \right)^{0.5} \tag{3}$$

where σ is the surface tension and f_s is the friction factor for flow over a smooth wall. Al-Sarkhi and Hanratty [15] expanded the measurement data for a horizontal annular flow. These experiments consisted of data for pipe dimensions of 2.54 cm and 9.53 cm. Ignoring the effect of liquid flow, an equation was developed similar to that of Tatterson:

Table 2
Froude numbers for horizontal stratified flow experiments.

Williams		REGARD		Mantilla	
j_G (m/s)	F_r (-/-)	j_G (m/s)	F_r (-/-)	j_G (m/s)	F_r (-/-)
26	26.94	19.8	12.91	21.0	29.71
31	32.12	24.9	16.23	30.0	42.43
37	38.34	34.4	22.43	51.0	72.14
45	46.63	38.2	24.90	70.0	99.01
67	69.43			84.0	118.82
88	91.20				

$$\left(\frac{\rho_g U_g^2 d_{50}}{\sigma} \right)^{0.36} \left(\frac{d_{50}}{D} \right)^{0.37} = 0.154 \tag{4}$$

Models of Tatterson and Al-Sarkhi and Hanratty differ in that exponents and constants are selected to match the scaling effects of the diameter and gas velocity on the droplet diameter. The exponential values may vary depending on which method of size characterization is used. The Sauter and volume median diameter data trend behaviors differ and scale differently according to the flow conditions. McCoy and Hanratty [8] chose to characterize the size of the droplets by the volume median diameter, defined such that droplets with diameters greater than this carry 50% of the volume. It was determined that this characterization, d_{50}, best describes the rate at which droplets deposit into the liquid film at the bottom of a pipe. Deposition rates were determined by studying the trajectory of injected particles of known size.

3.2. Droplet deposition literature review

The common practice for modeling deposition is to take the product of the deposition coefficient and the droplet concentration

$$\Gamma_D = k_D C_B = k_D \left(\frac{W_{LE}}{Q_G S} \right) \tag{5}$$

where Q_G is the volumetric flow rate of gas and S is the ratio of the droplet velocity to the gas core velocity. Another representation of droplet deposition rate can be given by

$$\Gamma_D = k_D' \frac{W_{LE}}{P} \tag{6}$$

where W_{LE} is the dispersed droplet mass flow rate and P is the perimeter, equal to πD for a pipe. The rate constant k_D' is the percent of liquid deposited in a unit length of pipe. Relating the constant k_D to k_D' can be seen by the following equation:

$$k_D' = \frac{4 k_D}{U_g D} \tag{7}$$

Namie and Ueda and McCoy and Hanratty observed the motion of very large droplets in annular flow and described it by a series of trajectories that originate at the liquid layer on the bottom wall. Some particle trajectories were intercepted at the top or side walls but most ended at the bottom wall, some distance downstream. To describe this trajectory motion for a horizontal flow, several studies have claimed that a coupling of the gravity term and turbulent diffusion terms is needed to determine the deposition coefficient. Williams suggests the drag force of the droplet be described by the Stokes law, which can be approximated as:

$$V_t = \frac{g d_d^2 \rho_l}{\mu_G} \tag{8}$$

The settling velocity term, V_t, is then used to describe the diffusion of droplets owing to the effects of gravity:

$$k_{gravity} = \frac{1}{\pi} V_t \int_0^\pi \frac{C_W}{C_B} \cos\theta d\theta \tag{9}$$

where C_W is the local concentration, C_B is the bulk concentration, and θ is the angle from the bottom of the cross section of the pipe. If the ratio between local and bulk concentrations is 1, then the droplet distribution is uniform, and gravity has little effect on deposition.

Williams proposes that at the top part of the pipe ($\theta > 90\,^\circ$), gravity is opposing deposition and at the bottom of the pipe ($\theta < 90\,^\circ$), gravity is aiding deposition. There is also an assumption made that there is no variation of droplet distribution along the vertical symmetric axis among the cross section, and thus, $180^\circ \geq \theta \geq 0^\circ$. He also states that $1 \geq (C_W/C_B) \geq 0$, where if the integral of $(C_W/C_B) = 1$, the gravitational settling top portion opposition would be balanced with the aiding lower portion. In addition, if the integral of (C_W/C_B) is larger at the bottom of the pipe, the portion of contribution that aids deposition would outweigh the opposing portion and possibly the turbulent diffusion term as well [9].

With regard to the modeling of the turbulent diffusion term, Williams' study was based on the study by Binder and Hanratty [13] study for vertical flows. In prior observations for vertical annular flows, concentration profiles were uniform, and droplet deposition to the liquid film was controlled by free flight, rather than by turbulent diffusion. Describing this free flight rate, v, they assumed that one-half of the drops are moving toward the wall at a Gaussian distribution for which the average magnitude of v is $(v^2)^{0.5}(2\pi)^{-0.5}$. The resulting equation used to describe the deposition constant was given by

$$k_{diffusion} = \left(\overline{v^2}\right)^{0.5}\sqrt{\frac{1}{2\pi}} \tag{10}$$

where $(v^2)^{0.5}$ is the mean square of the fluctuations of the particle velocity in a direction perpendicular to the wall.

Adjusting for horizontal flows, Williams adopted the diffusion term and coupled it with a term accounting for the effects of gravity. The coupled deposition constant equation that accounts for concentration profiles was suggested as follows:

$$k_D = \frac{C_W}{C_B}\left[\left(v^2\right)^{0.5}(2\pi)^{-0.5} + V_t\cos\theta\right] \tag{11}$$

Williams' proposed modeling basis for horizontal flows suggests that two terms are coupled, gravity and turbulent diffusion. The deposition behavior in previous studies was derived from vertical pipe flow experiments using a single term governed by a droplet free flight to wall; this does not suitably describe horizontal flows. Though the two-term deposition model suggested seems to be physical, there is no insight offered in this study on how to determine the distributions of the droplet concentrations in a pipe from the flow conditions.

To consider the concentration profiles of droplets in horizontal flows, the rate of deposition can be modified as follows:

$$\Gamma_D = k_D\left(\frac{C_w}{C_B}\right)C_B = k_D\frac{C_w}{C_B}\left(\frac{W_{LE}}{Q_G S}\right) \tag{12}$$

Accounting for the local concentration variance among the spatially averaged pipe section, the rate of deposition is given as

$$\langle \Gamma_D \rangle = \left\langle k_D\frac{C_w}{C_B}\right\rangle\frac{W_{LE}}{Q_G S} \tag{13}$$

Pan and Hanratty suggest gravitational settling as a major contributor to droplet deposition under flow conditions where gas velocities are low. The rate of deposition in Eq. (13) can be further simplified by substituting the terminal velocity, V_t, for $\langle k_D\frac{C_w}{C_B}\rangle$:

$$\langle \Gamma_D \rangle = V_t\frac{W_{LE}}{Q_G S} \tag{14}$$

The effects of turbulent diffusion are ignored, such that

$$V_t \gg \left(\overline{v^2}\right)^{0.5} \tag{15}$$

Here, the deposition is assumed to be completely controlled by gravitational settling. The settling velocity, V_t, is represented by Eq. (8) and is a function of droplet diameter size. These parameters are then used for this study's suggested deposition model, Γ_D, represented by Eq. (14).

3.3. Droplet entrainment modeling literature review

The rate of atomization for vertical flows with small liquid flow rates was first proposed by Dallman et al. [16]. The equation is given as follows:

$$\Gamma_E = k_A\frac{W_{LF} - W_{LFC}}{\sigma P}\left(\rho_g\rho_l\right)^{1/2}U_g^2 \tag{16}$$

where W_{LFC} is the critical film flow rate below which atomization does not occur. The rates of atomization will also differ between vertical and horizontal flows. This is due to asymmetries of the liquid layer in horizontal flows, leading to different atomization rates around the perimeter. If $\Gamma(\theta)$ equals the flow in the wall film per unit length at a given position along the perimeter, then the local rate of atomization is given as:

$$\Gamma_E = k_A\frac{\Gamma - \Gamma_c}{\sigma}\left(\rho_g\rho_l\right)^{1/2}U_g^2 \tag{17}$$

For $\Gamma \leq \Gamma_c$, the rate of atomization is zero. Integrating the atomization rate around the perimeter, Γ_E is defined by

$$\Gamma_E = \frac{1}{\pi D}\int_0^\pi D\Gamma_E d\theta \tag{18}$$

Solving Eq. (18) for the integral is equivalent to

$$\langle \Gamma_E \rangle = k_A\frac{\left(\rho_g\rho_l\right)^{1/2}U_g^2}{\sigma}\left[\frac{W_{LF}}{P} - \Gamma_c^*\right] \tag{19}$$

where

$$\Gamma_c^* = \Gamma_c - \frac{1}{\pi}\int_0^\pi(\Gamma_c - \Gamma)d\theta \tag{20}$$

When $\Gamma = \Gamma_c$, the angular location is defined by $\theta = \theta_c$. If $\Gamma > \Gamma_c$ around the whole perimeter, then $\theta_c = \pi$ and $\Gamma_c^* = \Gamma$. In addition, when $\Gamma < \Gamma_c$ over a portion of the perimeter from θ_c to π, then $\Gamma_c^* < \Gamma$. The rate of liquid flow at which atomization is initiated can be used to calculate the liquid critical flow rate per unit length, $\Gamma_c = W_{LFC}/\pi D$. This rate is given by

$$Re_{LFC} = 4\Gamma_c/\mu_l \tag{21}$$

Andreussi et al. [17] determined that $Re_{LFC} = 370$ for air and water at standard conditions. Other experiments show different values for the magnitude of Γ_c; however, the author neglected these effects due to the lack of a relation that can represent these differences. Consequently, Eq. (21) was used to determine the critical atomization rate and $\Gamma_c^* = \Gamma$.

4. Proposed models for droplet behavior

This section is dedicated to providing entrainment and deposition models that can be implemented in numerical simulation codes. Γ_E and Γ_D represent the interchange of droplets in a unit volume. These source terms are integrated over the interfacial area, which consists of an interface shape of the liquid film-gas core boundary and the length course of a pipe. Modeling for interfacial areas can influence developing lengths and is provided in the following sections.

4.1. Droplet size modeling

For reasons mentioned in the literature review, this study has chosen volume median diameter to represent the terminal velocity term used for the deposition modeling. With the addition of experimental measured droplet size data from a recent study on REGARD, a new model is suggested that follows the scaling effects of pipe diameter and gas velocity:

$$\left(\frac{\rho_g U_g^2 d_{50}}{\sigma}\right)^{0.13}\left(\frac{d_{50}}{D}\right)^{1.1} = 0.0013 \tag{22}$$

Solving for the droplet median volume diameter term, Eq. (22) gives the following:

$$d_{50} = \frac{0.0013 D^{1.1}\sigma^{0.13}}{U_g^{0.26}\rho_g^{0.13}} \tag{23}$$

Results of Eq. (22) calculations can be seen in Fig. 1. The figure also provides comparison data for experimental measured values and model calculations from Eq. (4) for various pipe dimensions. For the purpose of experimental data confidentiality, the droplet diameters (y-axis) are normalized.

Experiment data and model calculations both show an increase of drop size with increasing pipe diameter. It is interesting to note that the experimental data of REGARD show an increasing trend of droplet size with increasing gas velocity, whereas other experiments showed an inverse relationship. Valette and Henry [6] attribute this abnormal behavior to REGARD having a considerable number of small droplets vaporized when in contact with the gas core. The range of experimental measurements for the droplet size is limited in horizontal pipes; therefore, predictions outside these conditions should be considered when modeling the deposition rate.

4.2. Droplet deposition modeling

Values obtained for the droplet volume median diameter model are implemented in the terminal velocity given by Eq. (8), $V_t = \frac{gd_d^2\rho_l}{\mu_G}$. Terminal velocity calculations are then substituted in the suggested deposition model of this article, given as:

$$\Gamma_D = V_t\frac{W_{LE}}{Q_G S}. \tag{24}$$

As mentioned in the previous section, this model is applicable in cases in which the Froude number does not exceed 190. The ratio between the gas core and the droplet velocities S, was shown to be close to unity in the REGARD experiment data. Apart from this facility, there were few experiments that measured droplet speeds in horizontal flows. Because droplet velocity is close to gas core velocity due to large interface area, it is reasonable to consider $S \cong 1$. In the simulation code calculations, this parameter can affect results
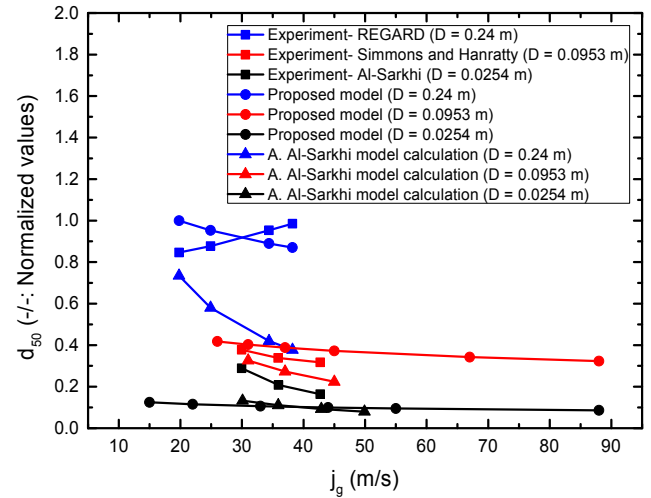

Fig. 1. Comparison between measurements of d_{50} from experiments and calculations with Equations (22) and (4).

of the droplet mass flow rates because the calculated gas and droplet velocities are used.

4.3. Droplet entrainment modeling

The onset of entrainment can be solved for as $\Gamma_c^* = 370\mu_l/4$ and the selected value for k_A in Eq. (19), provided by a correlation presented in the following section, gives this study's suggested entrainment rate as

$$\Gamma_E = 3.8 \times 10^{-7}\frac{\left(\rho_g\rho_l\right)^{1/2}U_g^2}{\sigma}\left[\frac{W_{LF}}{P} - \frac{370\mu_l}{4}\right] \tag{25}$$

These models for deposition and entrainment are suggested for simulation code systems. The following section details the derivation method used to obtain the entrainment coefficient, k_A

5. Correlation for droplet entrainment coefficient

To solve for the entrainment coefficient, k_A, an approach was made that correlates the balance of entrainment and deposition at fully developed flow. This approach was first explored by Williams and later expanded by Pan and Hanratty [5]. The application range is for flow conditions of. $U_g/\sqrt{Dg} < 190$.

Provided that the liquid viscosity is close to that of water, substitution of the k_D term from Eq. (5) into the k_D' relation, while assuming a fully developed flow, has been performed, i.e., $\Gamma_D = \Gamma_E$; the entrained fraction relation can be given as

$$\frac{(E/E_M)}{1-(E/E_M)} = \frac{k_A D U_g^3 S\left(\rho_g\rho_l\right)^{1/2}}{4k_D\sigma} \tag{26}$$

where k_A is a dimensionless constant, and the maximum entrainment, E_M, is given by:

$$E_M = 1 - \frac{W_{LFC}}{W_L} \tag{27}$$

Maximum entrainment is defined as the entrained fraction value that cannot be exceeded and for which a liquid film must exist at the bottom of a horizontal pipe. In past horizontal pipe experiments, it was observed that the entrained fraction at high gas velocities approaches unity but never reaches it. This trend is more
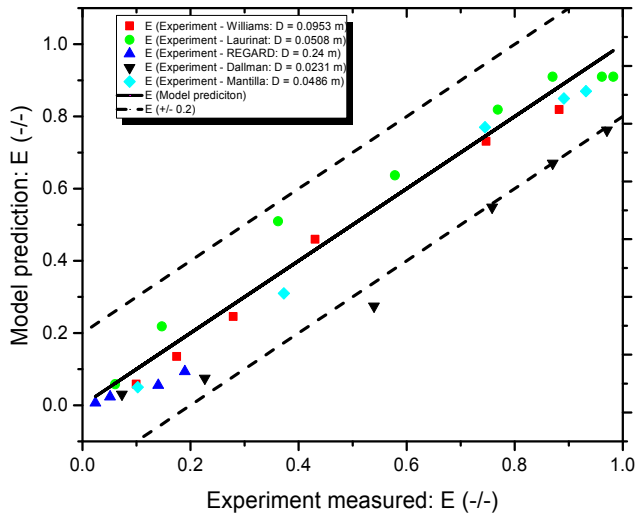
Fig. 2. Comparisons for entrained fraction E, obtained from the averaged values E/E_M, and measured data from experiments.

apparent at a high W_L because it is difficult to fully remove the liquid in a horizontal pipe. W_{LFC} is related to the maximum entrainment and is defined as the critical flow rate at which atomization is initiated. Pan and Williams used the following approach in correlating the entrained fraction modeling. The advancements of their work include modeling of the gravity effect in the deposition coefficient k_D. These studies recognized that gravity can cause asymmetric distributions of droplets in the gas phase. Asymmetries are less apparent at large enough gas velocities; however, in large diameter pipes, this condition is difficult to reach. Throughout all sets of experiments, the entrained fraction showed patterns of insensitivity to the parameter W_L, when flow conditions are such that W_L is not close to the critical liquid film rate, W_{LFC}. For this reason, a designated value for W_L, sufficiently larger than W_{LFC}, was selected to calculate the entrained fraction. Fig. 2 shows comparisons for entrained fraction E, obtained from the averaged values E/E_M, and measured data. The averaged values, $\langle E/EM \rangle$, are provided from the various experimental facilities mentioned in this study in Tables 3 and 4. It was found that $k_A = 3.8 \times 10^{-7}$ best suits

Table 3
Calculations for $\langle E/E_M \rangle$ = the average E/E_M for different liquid flows.

Williams (1990) W_L=0.64 kg/s		Laurinat (1984) W_L=0.31 kg/s		Dallman (1978) W_L=0.1134 kg/s	
U_g(m/s)	$\langle E/E_M \rangle$	U_g(m/s)	$\langle E/E_M \rangle$	U_g(m/s)	$\langle E/E_M \rangle$
26	0.061	18	0.064	15	0.04
31	0.135	24	0.240	22	0.098
37	0.245	34	0.560	33	0.360
45	0.460	44	0.700	44	0.720
67	0.731	57	0.900	55	0.880
		70	1.00	88	1.00
		103	1.00		
		131	1.00		

Table 4
Calculations for E/E_M = the average E/E_M for different liquid flows.

Mantilla (2008) W_L=0.19 kg/s		REGARD (2015) W_L=1.66 kg/s	
U_g(m/s)	$\langle E/E_M \rangle$	U_g(m/s)	$\langle E/E_M \rangle$
20.2	0.050	19.8	0.006
32.7	0.310	24.9	0.023
52.2	0.770	34.4	0.055
70.5	0.850	38.2	0.093
82.0	0.870		

the measured data from the different experiments. Fig. 2 shows the validity of the entrainment and deposition models; therefore, they were implemented into SPACE code.

The approach for developing an entrainment model in this study uses the same methodology as suggested in the study by Pan and Hanratty [5]. The novelty of this study is that it presents a new droplet diameter size model that considers the scaling effects with the inclusion of additional data from the latter study, REGARD. Changes to the diameter modeling affects the calculations for V_t which is used to represent the deposition constant, k_D. Consequently, the constant suggested for k_A is of a slightly different magnitude than that of Pan and Hanratty.

6. Validation results

This section presents the implementation of the deposition and entrainment modeling in the SPACE code. Fig. 3 is provided to show a sample SPACE nodalization of the REGARD experiment. Inlet and outlet boundary conditions are listed in Table 1. Pressures and temperatures were assumed to be constant between inlet and outlet.

6.1. Validation for fully developed flow

Fig. 4 is also provided to show comparisons of droplet mass flow rates from SPACE code calculations and experimental data for fully developed condition. The values for droplet mass flow rate have been normalized for data confidentiality, and the selected experiments chosen for SPACE simulation were by Williams, REGARD, and Mantilla. As mentioned before, discrepancies may exist between
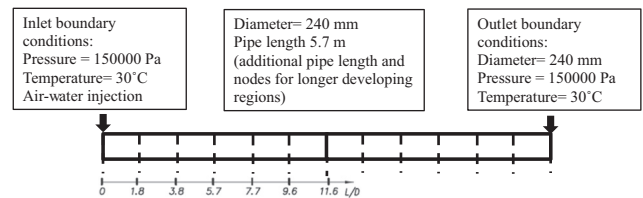

Fig. 3. REGARD pipe nodalization dedicated for SPACE validation.
SPACE, Safety and Performance Analysis Code for Nuclear Power Plants.
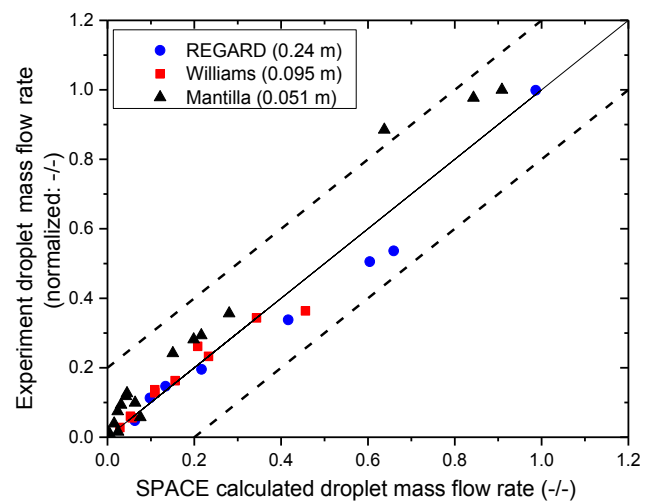

Fig. 4. Droplet mass flow rate comparisons between SPACE calculations and experimental measured data.
SPACE, Safety and Performance Analysis Code for Nuclear Power Plants.

Figs. 2 and 4 because the ratio of the gas core to the droplet velocities is assumed to be 1 in Eq. (24) for Fig. 2. Besides REGARD, all other experiments in this study have only measured data obtained at fully developed flow. Therefore, the furthest axial distance measurement data point (L/D = 11.6) was chosen to include for data comparisons in the REGARD experiment.

6.2. Validation for developing flow

The length along the axial direction of a pipe should be considered for successful modeling of the entrainment in a PWR hot leg. At a fully developed flow, the entrainment rate is equal to the droplet deposition rate, such that:

$$\frac{\partial \dot{m}_d}{\partial x_{|x \to \infty}} = 0 \Leftrightarrow \Gamma_E = \frac{k_D \dot{m}_d}{U_d \pi R^2} \tag{28}$$

This entrainment rate assumes that the rate does not change over the length of the pipe. To reach mass flow rates equal to those in the same developing regions as used in the REGARD experiment, entrainment rates must have a minimum magnitude. REGARD showed trends of rapid development of the droplet mass flow rates before the first measured location on the axial length of the pipe. Droplet mass flow rates showed a behavior in which they did not increase much beyond the first axial measurement locations. Therefore, it can be assumed that entrainment rates must have a high magnitude and that deposition does not have as much effect in the developing region. Fig. 5 provides a visual representation of how entrainment rates can be deduced based on developing length.

The entrainment rate is determined by assuming that the deposition rate is negligible between the initiation of two-phase flow (L/D = 0) and the time at which the first axial location is analyzed (L/D = 3.8). The initial slope of the droplet mass flow rates can be representative of the entrainment, as in:

$$\Gamma_E = \frac{\dot{m}_d(3.8) - \dot{m}_d(0)}{A_i(0 \to 3.8)} \tag{29}$$

The mass flow rates and interfacial areas are experimentally measured at axial locations. Droplets atomized in regions in which deposition is negligible will eventually be deposited over the course of the length of the pipe. In reality, deposition effects exist from the onset of two-phase flow; however, the droplets may experience an upward trajectory for a short period before the droplets reach the liquid interface at the bottom of the pipe. Therefore, entrainment rates can be more accurately obtained by measuring closer to the starting point of two-phase flow [6]. Pipe
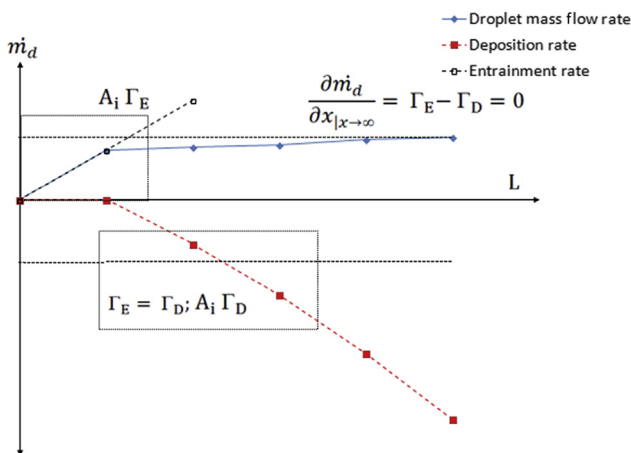
entrance effects also affect the developing region for the mass flow exchange of liquid film and droplets. The interfacial area of the liquid film can influence the developing length; therefore, this parameter should also be considered. Owing to several unknown variables that are associated with this phenomenon (i.e., injection nozzle type, angle of injection, etc.), the prediction of an appropriate developing length region is very difficult.

Fig. 6 presents comparisons for deduced entrainment rates from the REGARD experiment against Eq. (25) calculations from SPACE. Although the entrainment models were developed without consideration of the developing length, it is interesting to see that the model predictions are in good agreement with the measured values.

The point at which a fully developed flow is reached is when the net contribution for the deposition and entrainment are balanced and the mass flow rate of droplets has fully developed. To show the effects of interfacial area on the developing length over the course, two interface geometries are chosen. Neither of these interfaces is physical because wavy interfaces are not accounted for; however, they still provide insight into the sensitivity of the interfacial area parameter to developing length. The suggested equation used to represent the interfacial area for a straight horizontal interface is given as:

$$A_i = D^* \sin \theta^* L_{cell} \tag{30}$$

where L_{cell} is the length of a specified cell in a control volume. In addition, annular flow interfacial area is given by:

$$A_i = \pi D^* L_{cell}^* \sqrt{1 - \alpha_l} \tag{31}$$

Geometric representations for these parameters are given in Figs. 7 and 8. In Figs. 10 and 12, the results for the SPACE calculations, using a straight interface, are compared with experimental measured results for REGARD. Figs. 9 and 11 present the results of the SPACE calculations using an annular interface.

The source terms for droplet deposition and entrainment relations were implemented in SPACE and are in good agreement with experimental results when fully developed conditions are achieved. REGARD has been validated for a developing flow, and a combination of 40 data set points exists from this experiment. The SPACE calculations for straight interfaces show longer developing lengths than experimental measurements at high gas velocities. For
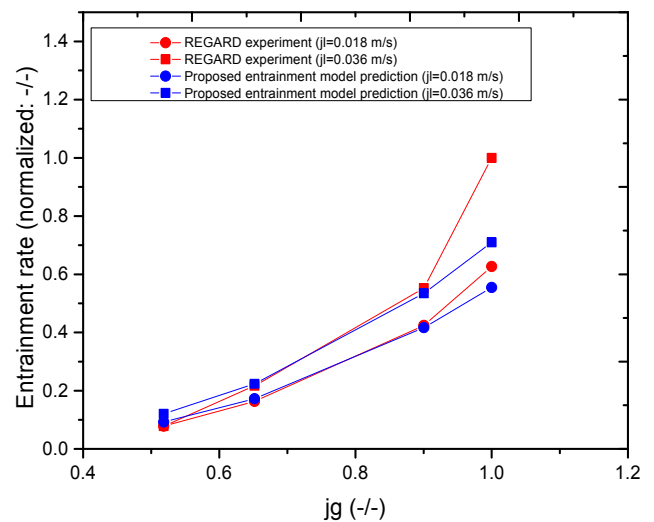

Fig. 5. Method for droplet entrainment assessment.

Fig. 6. Comparisons of Equation (25) calculations with k_A=3.0×10^{-7} and REGARD experiment measured entrainment rates.
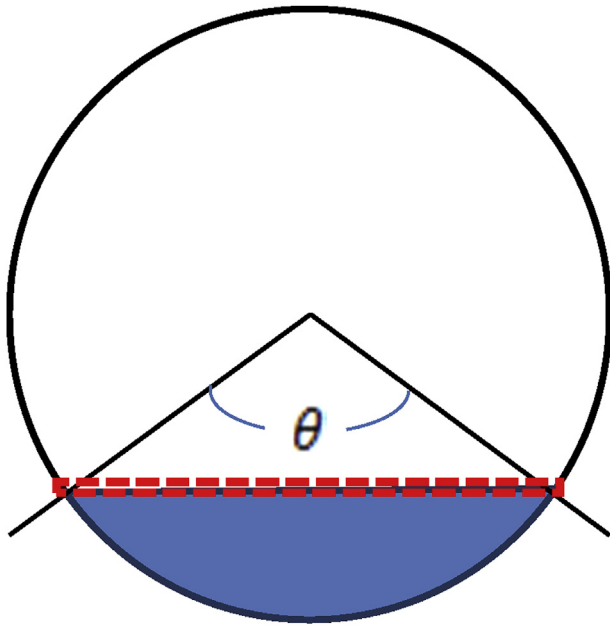
Fig. 7. Interfacial area for horizontal stratified flow (red line).
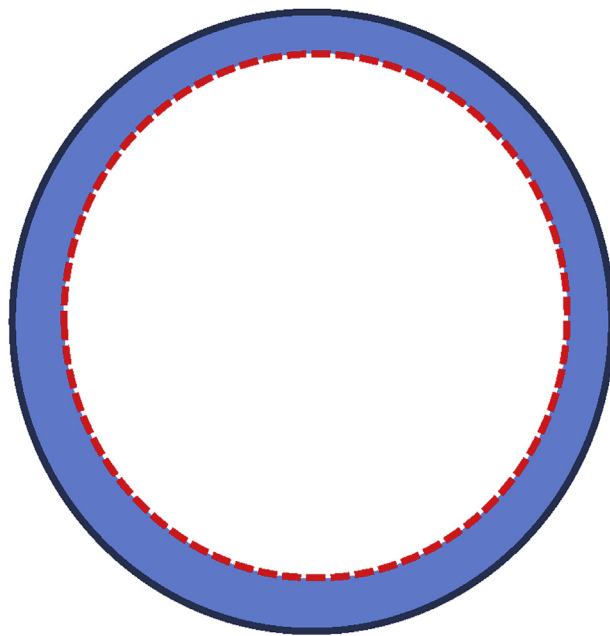

Fig. 8. Interfacial area for horizontal annular flow (red line).

conditions in which the gas velocities are low, the developing region predicted by the straight interface model is in good agreement with experimental data. Perhaps the differences in developing lengths can be attributed to wavy effects and asymmetries being more apparent under high gas velocities. Several other parameters may influence the prediction of the interfacial area term, such as liquid film holdup, pressure drops, etc. It can be seen that the interfacial area term significantly impacts the developing region length.

7. Discussion and future work

This study relies on the correct prediction of the droplet diameter size in determining the gravitational settling velocity term
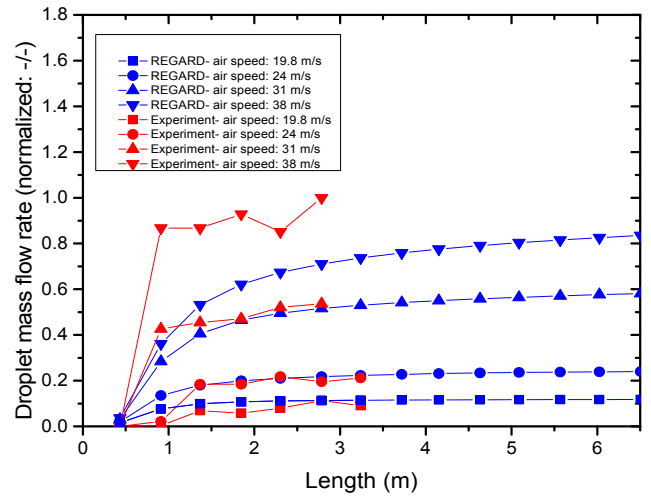

Fig. 9. Data for droplet mass flow rates along the axial location of a horizontal pipe at injection rate W_L=1.66 kg/s. REGARD comparisons between experimental measurement data and SPACE calculations where interfacial area is calculated from Equation (31). SPACE, Safety and Performance Analysis Code for Nuclear Power Plants.
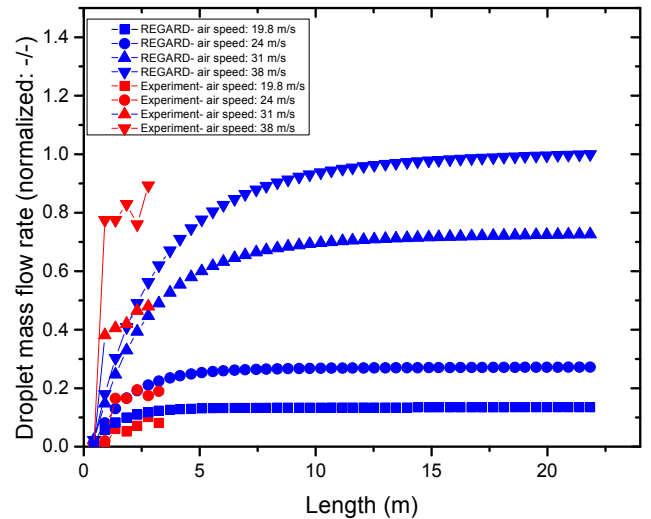

Fig. 10. Data for droplet mass flow rates along the axial location of a horizontal pipe at injection rate W_L=1.66 kg/s. REGARD comparisons between experimental measurement data and SPACE calculations where interfacial area is calculated from Equation (30). SPACE, Safety and Performance Analysis Code for Nuclear Power Plants.

used to model the droplet deposition rate. The droplet deposition rate is assumed in this model to be completely controlled by the settling velocity. Previous deposition studies have shown that the velocity at which droplets intercept the bottom wall of a horizontal pipe may be of a smaller magnitude than that of the settling velocity. Despite these differences, the empirical correlation suggested by Pan and Hanratty [5] was modified by the inclusion of the larger scale experiment, REGARD. The REGARD experiment provides droplet diameter size data, and therefore, the scaling effects of the pipe diameter and gas velocity could be accounted for. Owing to the limited range of available experiments on horizontal flow, the application range of this model is not guaranteed outside of these experimental conditions and pipe dimensions.

Previous and ongoing studies exist for a mechanistic wave model for the entrainment rate; however, there has been no model yet that can be successfully validated with laboratory data for
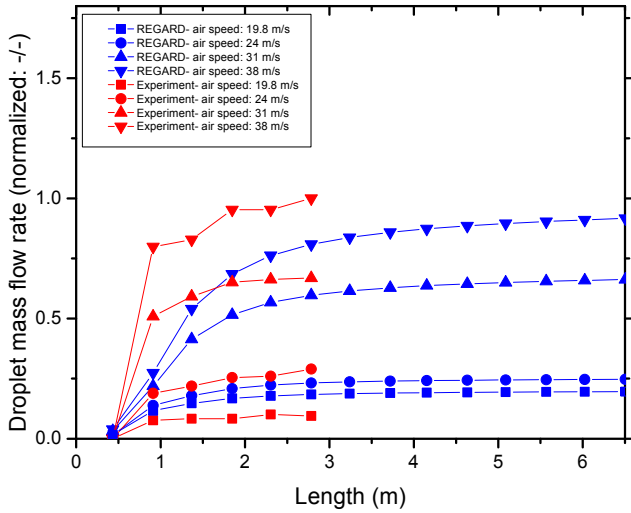
Fig. 11. Data for droplet mass flow rates along the axial location of a horizontal pipe at injection rate W_L=0.83 kg/s. REGARD comparisons between experimental measurement data and SPACE calculations where interfacial area is calculated from Equation (31). SPACE, Safety and Performance Analysis Code for Nuclear Power Plants.

Fig. 12. Data for droplet mass flow rates along the axial location of a horizontal pipe at injection rate W_L=0.83 kg/s. REGARD comparisons between experimental measurement data and SPACE calculations where interfacial area is calculated from Equation (30). SPACE, Safety and Performance Analysis Code for Nuclear Power Plants.
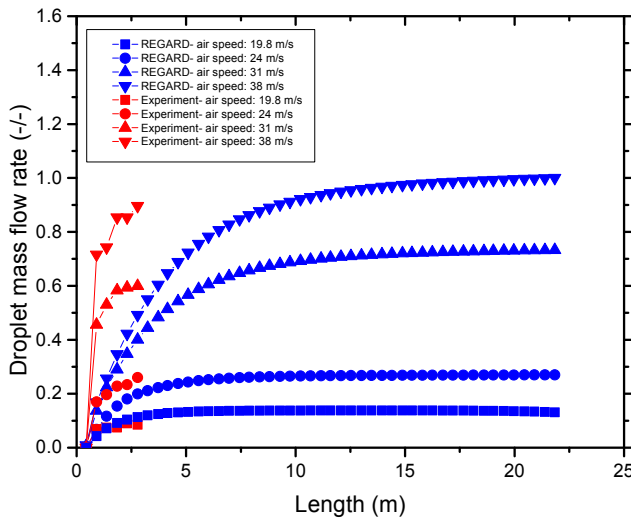
different pipe dimensions. Perhaps more investigation is this field can produce a more accurate entrainment model. The effects of scaling of the entrainment rate with the pipe diameter should carefully be considered.

Deposition modeling can be furthered using Pan and Hanratty's theoretical approach considering concentration profiles and droplet size distributions. The second approach was a theoretical analysis of particle turbulence, and gravity effects were used to obtain a general relation for the droplet deposition. The gravity term also considers the droplet concentration profiles and droplet size distribution. This model is applicable for both large and small droplets $U_g/\sqrt{Dg}$.

In this approach, the gravity term becomes less dominant, and turbulent diffusion forces control the deposition as the concentration becomes more symmetrical. In the scope of this study, the application of these models was limited to a horizontal flow in which the gravity term is assumed to be in full effect.

The entrainment modeling suggested in this article is in good agreement with measured data under fully developed conditions. Understanding a way to measure and model developing flow region phenomena is important for PWR hot leg accident simulation. Experimental facilities cover only air—liquid flows; however, steam—liquid flows are experienced during a real PWR hot leg accident scenario. Droplet behavior differences between air—gas and steam—liquid flow should be considered. Several factors mentioned in this article are probable contributors affecting the developing length for droplet entrainment. Modeling of a wavy liquid film interfacial area as a function of the gas velocity could help improve predictions for developing flows

Conflicts of interest

All authors have no conflicts of interest to declare.

Acknowledgment

Nomenclature

A_i	Liquid—air interface area
C_B	Bulk droplet concentration
C_W	Local droplet concentration
D	Pipe diameter
d_{50}	Volume median diameter
d_d	Droplet diameter
E	Entrained fraction
E_M	Maximum entrained fraction
F_r	Froude number
f_s	Friction factor over smooth wall
g	Gravitation constant
j_g	Superficial gas velocity
k_A	Droplet entrainment coefficient
k_D	Deposition coefficient
k'_D	Percent of liquid deposited in a unit length of pipe
$k_{diffusion}$	Droplet deposition coefficient due to turbulent diffusion
$k_{gravity}$	Droplet deposition coefficient due to gravity
L_{cell}	Length of control volume cell
$\dot{m}_d$	Mass flow rate of entrained droplets
P	Pipe perimeter
Q_G	Volumetric gas flow rate
Re_{LFC}	Reynolds number with liquid flow rate at which atomization is initiated
S	Ratio of the droplet velocity to the gas core velocity
U_g	Gas phase velocity
v	Particle velocity
V_t	Gravity drag force
W_L	Liquid phase mass flow rate
W_{LE}	Mass flow rate of the entrained liquid
W_{LF}	Liquid film mass flow rate
W_{LFC}	Critical liquid film mass flow rate

Symbols

α_l	Liquid film volume fraction
Γ_c	Critical atomization rate
Γ_D	Droplet deposition rate

Γ_E	Droplet entrainment rate
μ_d	Droplet liquid phase dynamic viscosity
μ_g	Gas phase dynamic viscosity
μ_l	Liquid phase dynamic viscosity
ρ_g	Gas phase density
ρ_l	Liquid phase density
σ	Surface tension

Acronyms

LOCA	Loss of Coolant Accident
SPACE	Safety and Performance Analysis Code

References

[1] J.K. Schimpf, K.D. Kim, Droplet entrainment and deposition in horizontal stratified two-phase flow. World Academy of Science, Engineering and Technology (WASET), Int. J. Nucl. Quant. Eng. 4 (5) (2017).

[2] L.R. Williams, Effect of Pipe Diameter on Horizontal Annular Two-Phase Flow, Ph.D. Dissertation, University of Illinois at Urbana-Champaign, 1990.

[3] J.C. Dallman, Investigation of Separated Flow Model in Annular Gas-liquid Two-phase Flows, Ph.D. thesis, University of Illinois, Urbana, IL, 1978.

[4] J.E. Laurinat, T.J. Hanratty, W.P. Jepson, Film thickness distribution for gas-liquid annular flow in a horizontal pipe, PCH Physicochem. Hydrodyn. 6 (1–2) (1984) 179–195.

[5] L. Pan, T.J. Hanratty, Correlation of entrainment for annular flow in horizontal pipes, Int. J. Multiphas. Flow 28 (2002) 385–408.

[6] M. Valette, F. Henry, Droplet Entrainment Over a Stratified Flow in a PWR Hot Leg: Results of the REGARD Experiment, CEA, 2015.

[7] I. Mantilla, Mechanistic Modeling of Liquid Entrainment in Gas in Horizontal Pipes, Ph.D. Dissertation, University of Tulsa, 2008.

[8] D.D. McCoy, T.J. Hanratty, Rate of deposition of droplets in annular two-phase flow, Int. J. Multiphas. Flow 3 (1975) 319–331.

[9] L. Williams, L. Dykhno, T. Hanratty, Droplet flux distributions and entrainment in horizontal gas-liquid flows, Int. J. Multiphas. Flow 22 (1) (1996) 1–18.

[10] L.G. Alexander, C.L. Coldren, Droplet transfer from suspending air to duct walls, J. Ind. Eng. Chem 43 (1951) 1325–1331.

[11] S. Namie, T. Ueda, Droplet transfer in two-phase annular mist flow, Bull. Jpn. Soc. Mech. Eng. 15 (1972) 1568.

[12] R.J. Anderson, T.W.F. Russell, Film formation in two-phase annular flow, AIChE (Am. Inst. Chem. Eng.) 14 (1970) 626–633.

[13] J.L. Binder, T.J. Hanratty, Use of Lagrangian methods to describe drop deposition and distribution in horizontal gas-liquid annular flows, Int. J. Multiphase. Flow 18 (1992) 803–820.

[14] D.F. Tatterson, J.C. Dallman, T.J. Hanratty, Drop sizes in annular gas-liquid flows, J. AIChE (Am. Inst. Chem. Eng.) 23 (1977) 68–76.

[15] A. Al-Sarkhi, T. Hanratty, Effect of pipe diameter on the drop size in a horizontal annular gas–liquid flow, Int. J. Multiphas. Flow 28 (10) (2002) 1617–1629.

[16] J.C. Dallman, B.G. Jones, T.J. Hanratty, Interpretation of entrainment measurements in annular gas–liquid flows, in: F. Durst, G.V. Tsiklauri, N.H. Afgan (Eds.), Two-Phase Momentum, Heat and Mass Transfer, vol. 2, Hemisphere, Washington, DC, 1979, pp. 681–693.

[17] P. Andreussi, J. Asali, T.J. Hanratty, Initiation of roll waves in gas–liquid flows, J. AIChE (Am. Inst. Chem. Eng.) 31 (1985) 126.